https://doi.org/10.5194/acp-2019-950
Preprint. Discussion started: 16 December 2019

Atmospheric Chemistry and Physics Discussions

Craig-Gordon model validation using observed meteorological parameters and measured stable isotope ratios in water vapor over the Southern Ocean

Shaakir Shabir Dar[1], Prosenjit Ghosh[1,2], Ankit Swaraj[2], and Anil Kumar[3]

[1]Centre for Earth Sciences, Indian Institute of Science, Bengaluru, 560012, Karnataka, India.
[2]Divecha Centre for Climate Change, Indian Institute of Science, Bengaluru, 560012, Karnataka, India.
[3]National Centre for Polar and Ocean Research, Vaso-da-Gama, 403804, Goa, India.

Correspondence: Prosenjit Ghosh (pghosh@iisc.ac.in)

Abstract. The stable isotopic composition of water vapor over the ocean is governed by the isotopic composition of surface water, ambient vapor isotopic composition, exchange and mixing processes at the water-air interface as well as the local meteorological conditions. In this study we present water vapor and surface water isotope ratios in samples collected across the latitudinal transect from Mauritius to Prydz Bay in the Antarctic coast. The samples were collected on-board the ocean research vessel SA Agulhas during the 9^{th} (Jan-2017) and 10^{th}(Dec-2017 to Jan-2018) Southern Ocean expeditions. The inter annual variability of the meteorological factors governing water vapor isotopic composition is explained. The parameters governing the isotopic composition of evaporation flux from the oceans can be considered separately or simultaneously in the Craig-Gordon(CG) models. The Traditional Craig-Gordon (TCG) (Craig and Gordon, 1965) and the Unified Craig-Gordon (UCG) (Gonfiantini et al., 2018) models were used to evaluate the isotopic composition of evaporation flux for the molecular diffusivity ratios suggested by (Merlivat, 1978)(MJ), (Cappa et al., 2003)(CD) and (Pfahl and Wernli, 2009)(PW) and for different ocean surface conditions. We found that the UCG model with CD molecular diffusivity ratios where equal contribution from molecular and turbulent diffusion is the best match for our observations. By assigning the representative end member isotopic compositions and solving the two-component mixing model, a relative contribution from locally generated and advected moisture was calculated along the transect. Our results suggest varying contribution of advected westerly component with an increasing trend up to 65°S. Beyond 65°S, the proportion of Antarctic moisture was found to be increasing linearly towards the coast.

1 Introduction

The knowledge of factors governing evaporation of water from the oceans is an essential part of our understanding of the hydrological cycle. Nearly ≈ 97% of the water of earth is in the oceans as saline while the residual ≈ 3% is fresh water stored in groundwater, glaciers and lakes, or flowing as rivers and streams (Korzoun and Sokolov, 1978). Evaporation of ocean water generates vapour and forms the initial ingredient in the hydrological cycle. A fraction of this vapor, only ≈ 10% of it is transported inland to the continent and generate precipitation, while rest of the moisture precipitates over the ocean (Oki

https://doi.org/10.5194/acp-2019-950
Preprint. Discussion started: 16 December 2019

Atmospheric Chemistry and Physics Discussions

and Kanae, 2006; Shiklomanov, 1998). The oceans regulate the global climate of the earth through heat and moisture transport (Chahine, 1992). Measurements of the isotope composition of water in the various components of the water cycle over the ocean offers useful tool to derive information about the origin of water masses and understanding of the physical mechanisms involved during its genesis, transport and finally precipitation (Craig, 1961; Dansgaard, 1964; Yoshimura, 2015; Gat, 1996; Araguás-Araguás et al., 2000; Noone and Sturm, 2010; Gat et al., 2003; Benetti et al., 2014; Galewsky et al., 2016).

The isotopic composition of vapor on top of a water body is governed by: i) Thermodynamic equilibrium process responsible for the phase transformation at a particular temperature ii) Kinetic or non-equilibrium processes where role of wind is significant and iii) Large-scale transport and mixing: due to the movement of air parcels laterally and vertically. Initially a two-layer model to capture the isotopic composition of evaporated flux was proposed (Craig and Gordon, 1965) and subsequently modified (Gonfiantini et al., 2018). The CG model incorporates the equilibrium and kinetic processes to deduce the isotopic composition of air packet. However, to get a more realistic picture of the hydrological cycle over the ocean, the horizontal transport and advective mixing is important and should be incorporated.

Comparatively large volume of data exists over land to understand the terrestrial hydrological cycle and through the Global Network in Precipitation(GNIP) initiative of the International Atomic Energy Agency (IAEA). However, only a handful records of spatial and temporal variability of precipitation and vapor isotopic composition over the oceans is available for any assessment (for example the Indian Ocean and the Southern Ocean(Uemura et al., 2008; Rahul et al., 2018; Prasanna et al., 2018), the Atlantic Ocean(Benetti et al., 2017b, a, 2015) and Mediterranean Sea (Gat et al., 2003)) and hence further effort is needed to enhance the spatial and temporal coverage. In this paper we present stable isotope ratios in water vapor and ocean surface water samples from locations covering diverse oceanic settings; i.e. tropical, subtropical and polar latitudes, with a large range in the sea surface temperature, relative humidity and wind speed noted during the time of expeditions. In this study we identified the controls governing the isotopic composition of water vapor. Further we evaluated the sampling strategy i.e. sampling at two heights above the sea level to determining the isotope ratios in the water vapor. The performance of the Craig-Gordon evaporation models in diverse ocean conditions was evaluated in the context of estimation of the contribution of advected vs in-situ derived vapor for different zones over the Southern ocean.

2 Sampling methods and isotopic measurements

The samples (water vapor, and surface water) for this study were collected along the stretch from Mauritius to Prydz Bay (24°S to 69°S and 57°E to 76°E) during the Austral Summer covering the months of January 2017 (SOE-IX) and December 2017 to January 2018 (SOE-X) onboard SA Agulhas. The water vapor sampling inlets were set at two heights above the mean sea level. An aggregate of 71 water vapor samples at a height of $\approx$ 15m (Nwv) above the sea level and 19 water vapor samples (Swv) were collected close to the sea surface. The Swv samples were collected at the boundary layer during the calm ocean surface condition. Fig. 1 shows the sampling locations locations. Alongside water vapor, 49 surface water samples were also collected. The details about the sampling procedures for collection of water vapor and surface water samples are given in the supplementary document. All these subjected to isotopic analysis the details of which are also provided in the supplementary

https://doi.org/10.5194/acp-2019-950
Preprint. Discussion started: 16 December 2019

Atmospheric Chemistry and Physics Discussions

document. The isotope ratios are expressed in ‰ using the standard δ notation relative to Vienna Standard Mean Ocean Water (VSMOW).

3 Results

3.1 Meteorological observations and air mass trajectories

Along with the samples in-Stu and real-time meteorological data such as Relative Humidity(h), Wind Speed (ws), Air Temperature (Ta), Sea Surface Temperature (sst), and Atmospheric Pressure (P) were recorded during the expedition. Fig. 2 shows the latitudinal variation of these meteorological parameters. A wide range of these physical parameters are observed since the sampling transect encompasses diverse oceanic settings.

The sampling locations can be broadly categorised into zones which are designated with different wind patterns (i.e. velocity and the moisture carrying capacity). We identified westerlies and polar easterlies based on 72 hour back-trajectories constructed at three different heights in the atmospheric boundary layer. 3-day backward air mass trajectories were determined by the Hybrid Single Particle Lagrangian Integrated Trajectory (HYSPLIT) model (Draxler and Hess, 1998; Stein et al., 2015) with NOAA-NCEP/NCAR Re-analysis 2 (Kanamitsu et al., 2002) results as an input. HYSPLIT is a computational model hybrid between Lagrangian and Eulerian method of calculating advected and diffusive air masses. It generates 3-D back trajectories of air parcels and meteorological variables such as temperature, relative humidity, specific humidity, rainfall, pressure etc. along the path of air trajectories. Fig. 3 shows the back trajectories for the water vapor sampling locations. During the SOE X expedition, the change is trajectory from trade winds to westerlies was at ≈31°S and at ≈63°S , change from westerlies to polar easterlies is seen. For SOE IX the transition from the westerlies to easterlies and then to polar westerlies were documented at the ≈33°S and ≈64°S latitudes respectively.

3.2 Isotopic measurements along the transect

$\delta^{18}O$ of surface water was heavier (> 0 ‰) until ≈ 40°S latitude. A transition to lighter water was observed beyond ≈ 45°S latitude with a major drop documented in the surface water isotopic values on approaching the coastal Antarctica. Fig. 4 show the latitudinal variation of $\delta^{18}O_{sw}$ plotted and compared with data extracted from the Global Sea Water 18O Database (Schmidt et al., 1999). The transition zone was demarcated with a sst value of 17°C at ≈43.6°S latitude to sst of 12°C at ≈45°S latitude during SOE IX, while a similar drop in the sst values i.e. from 16.5°C at ≈40°S latitude to 11.0°C at ≈ 42°S latitude for the expedition SOE X. These sst and $\delta^{18}O_{sw}$ values marking the zones were earlier defined based on surface seawater isotope and salinity data (Srivastava et al., 2007; Tiwari et al., 2013). These zones divided based on the distinct regions in the Southern Ocean with varying conditions of evaporation, precipitation or melting and freezing. The different zones were marked as: i) Zone of evaporation (North of ≈4.5°S and ≈20°S-41°S), zone of precipitation (≈4.5°S-20°S) iii) Zone of melting/freezing (≈47°S to ≈ 68°S). The region between the evaporation and melting/freezing regions, i.e. ≈41°S-47°S, is designated as the transition zone.

https://doi.org/10.5194/acp-2019-950
Preprint. Discussion started: 16 December 2019

Atmospheric Chemistry and Physics Discussions

The $\delta^{18}O_{Nwv}$ and $\delta^{2}H_{Nwv}$ in water vapor samples collected at an height of ≈ 15m (Nwv) above sea level showed a expected trend across latitude for both the expeditions. The vapor isotopic composition is seen to be gradually dropping with higher latitudes. A steady drop was noted from ≈30°S to ≈65°S and a sharp change in the gradient was registered at ≈65°S, where lighter lighter water vapor isotopic composition was evident. Extreme lighter values were recorded on approaching ≈65°S, where mixing of the moisture packet carrying lighter continental vapor from the Antarctica (Uemura et al., 2008) was attributed. The $\delta^{18}O_{Nwv}$ ($\delta^{2}H_{Nwv}$) of water vapor varies from -10.9‰ (-80.8‰) to -27.5‰(-221.4‰) respectively. There are deviations from this general trend with heavier isotopic composition observed at the higher(lower) latitudes. The variations can be accounted, by taking into consideration the source and the path of air masses . The lighter values of vapor isotopic composition can be traced to the source being higher(lower) latitudes. The isotopic composition, $\delta^{18}O_{Swv}$ ($\delta^{2}H_{Swv}$) of the water vapor collected close to the surface (Swv) varies between -11.3 ‰(-88.1 ‰) to -21.55‰ (-163.75‰). These samples were collected during calm ocean surface conditions to negate the influence of sea spray.

Deuterium excess (dxs), defined as $dxs = \delta^{2}H - 8 \times \delta^{18}O$, is a second order isotope parameter. dxs in the water vapor correlates with the meteorological parameters at the ocean surface such as relative humidity, sea surface temperature and wind speed (Uemura et al., 2008; Rahul et al., 2018; Benetti et al., 2014; Midhun et al., 2013). Therefore, it serves as a proxy for the moisture source conditions. The dxs and relative humidity are strongly coupled, which is indirectly linked with the wind speed. The kinetic effect determined by the magnitude of moisture gradient between evaporating water surface and overlying unsaturated air. In other words, lower the relative humidity higher is the dxs. Wind speed regulates the turbulent vs molecular diffusion across the diffusive layer. The role of sst in governing the dxs is through the process of equilibrium fractionation, which is temperature dependent. The dxs values in water vapor range from 18.7‰ to -23.7‰ . A relatively higher dxs values in ocean water vapor comes from ≈25°S to ≈45°S with a slight step change to lower dxs values was recorded on approaching 45°S which extend until ≈65°S. Beyond ≈ 65°S a slight increment in the vapor dxs was observed as depicted in the box-plot in Fig. 4d. The statistics of the isotopic composition of water vapor is tabulated in Table 1.

3.3 Meteorological controls on the isotopic composition of water vapor

The $\delta^{18}O_{Nwv}$ and $\delta^{2}H_{Nwv}$ are positively correlated with sst. Fig. 5 shows the linear regression equations fitted with the data points, also included are data from (Uemura et al., 2008) for comparison. For all the water vapor samples, $\delta^{2}H_{Nwv}$ and $\delta^{18}O_{Nwv}$ are correlated with sst explaining ≈33% of the variance in $\delta^{18}O_{Nwv}$ and ≈50% of the variance in $\delta^{2}H_{Nwv}$. The strength of the correlation slightly higher if sampling from individual years is considered separately. In all cases for this study, the slope and intercept of the regression equation between the isotopic composition of water vapor and sst is comparable with Uemura et al. (2008) with higher correlation. Fig. 5b shows the regression equations neglecting samples with the influence of Antarctic vapor mixing as evident from the back trajectories i.e. samples collected north of 65°S. The isotopic composition of water vapor is uncorrelated with relative humidity. In Uemura et al. (2008), due to the absence of wind speed data, the role of wind speed in controlling the isotopic composition of water vapor was left un-assessed. Here we find that the relationship between $\delta^{2}H_{Nwv}$ vs wind speed was prominent as compared to the relationship between $\delta^{18}O_{Nwv}$ vs wind speed. This is true

https://doi.org/10.5194/acp-2019-950
Preprint. Discussion started: 16 December 2019

Atmospheric Chemistry and Physics Discussions

for samples collected north of ≈65°S Fig. 5. It can be concluded that the $\delta^2 H_{Nwv}$ is more sensitive to sst and wind speed as compared to $\delta^{18} O_{Nwv}$.

Fig. 6 shows the dependency of deuterium excess in vapor with the meteorological conditions. For samples collected north of 65°S , the linear regression equation of the relationship between dxs and relative humidity is dxs=0.56h+46.36 (r^2=0.49). These slope and intercept values were similar to the earlier reports documenting the isotope variability in water vapour from the Indian sector of the Southern Ocean (Uemura et al., 2008; Rahul et al., 2018) the Bay of Bengal (Midhun et al., 2013), the Atlantic (Benetti et al., 2014) and the Mediterranean (Gat et al., 2003). For samples collected south of 65°S the relationship become weaker. Surprisingly the strength of the dxs vs h relationship was stronger if data exclusively from a single expedition is considered separately with the slope and intercept of the regression equation for the SOE IX and SOE X expeditions are displayed as -0.64‰/%; 57.4‰ (r^2=0.77) and 0.64‰/%; 48.7‰ (r^2=0.61) respectively.The dxs in vapor is positively correlated with the sst and comparable with the linear regression fit recorded for the other oceans, namely Southern Ocean, Atlantic, Bay of Bengal. The linear regression equation for samples collected north of 65°S is given by dxs=0.70 * sst-4.65 (r^2=0.49). For samples collected north of 65°S the correlation the regression equation is given by dxs=-0.53 ws+11.65 (r^2=0.23). Our observations compliment the earlier studies suggesting the dependency of water vapor d-excess on relative humidity, sst and wind speed.

$\delta^{18} O_{Swv}$ and $\delta^2 H_{Swv}$ of the Swv samples are strongly correlated with sst ($\delta^{18} O_{Swv}$ = 0.37 sst-18.51 r^2=0.67; $\delta^2 H_{Swv}$ =2.45 sst-141.27 r^2=0.51). The slopes of these regression equations are higher than that of the Nwv samples, while the intercept is lower. The relationship was stronger between $\delta^{18} O_{Swv}$ vs sst for Swv samples as compared to the Nwv samples explained earlier. No correlation was observed between $\delta^{18} O_{Swv}$ of vapor and wind speed. Interestingly, the dxs of the Swv samples was only weakly correlated with relative humidity dxs= -0.57*h+49.22 (r^2=0.16). Even though the strength of correlation is weak, the slope and intercept of the dxs vs relative humidity regression equation was similar to the water vapour (Nwv) samples.

4 Discussion

4.1 Craig-Gordon (CG) model evaluation

Craig-Gordon 1965 (referred to as Traditional Craig-Gordon Model (TCG)) proposed the first theoretical model to explain the isotopic composition of water vapor during the process of evaporation. The isotopic composition of vapor generated from ocean water depends on the isotopic composition of the surface oceanic water, the isotopic composition of water vapor in the ambient atmosphere along with the relative humidity level at the site of sample collection. The interplay of equilibrium and kinetic fractionation between the phases governs the final isotopic composition in the water vapour and liquid. The equilibrium fractionation between ocean water and vapor is controlled by the sea surface temperature (sst). In comparison, relative humidity and wind speed control the the kinetic fractionation through the combination of molecular diffusion and turbulent diffusion. Molecular diffusion leads to isotopic fractionation between liquid and vapor whereas the turbulent diffusion is usually non-fractionating. To estimate the isotopic composition of water vapor CG model invokes two-layers; a laminar layer above the air-water interface where the transport process is active via molecular diffusion and a turbulent layer above the

https://doi.org/10.5194/acp-2019-950
Preprint. Discussion started: 16 December 2019

Atmospheric Chemistry and Physics Discussions

laminar layer in which the molecular transfer is predominantly by the action of turbulent diffusion. Assuming there is no divergence/convergence of air mass over the oceanic atmosphere, the isotopic ratio of the evaporation flux is given as Craig and Gordon (1965) (TCG):

$$R_{ev} = \alpha_k . \frac{R_L . \alpha_{eq} - h . R_A}{1 - h} \tag{1}$$

Based on most recent proposition Gonfiantini et al. (2018) proposed a modified version of the model, termed as Unified Craig-Gordon (UCG) model in which the parameters controlling the isotopic composition of the evaporation flux are considered simultaneously. From Gonfiantini et al. (2018), The net evaporation rate of liquid water(E) is the difference between the vaporization rate, ψ_{vap}, and the atmospheric vapor capture rate (i.e; condensation) by the liquid water, ψ_{cap}.

$$E = \psi_{vap} - \psi_{cap} = (\gamma - h)\psi^o_{cap} \tag{2}$$

Where the ψ^o_{cap} is the vaporization rate of pure water, h is the Relative Humidity and γ is the thermodynamic activity coefficient of evaporating water which is <1 for the saline solutions and 1 for the pure water or dilute solutions.

From eq. (2), We can write;

$$R_{ev}(\gamma - h)\Psi^o_{vap} = R_{esc}\gamma\Psi^o_{vap} - R_{cap}h\Psi^o_{vap} \tag{3}$$

$$R_{ev}(\gamma - h)\Psi^o_{vap} = \frac{R_L}{\alpha_{eq}\alpha^x_{diff}}\gamma\Psi^o_{vap} - \frac{R_A}{\alpha^x_{diff}}h\Psi^o_{vap} \tag{4}$$

$$R_{ev} = \frac{\frac{R_L}{\alpha_{eq}\alpha^x_{diff}}\gamma - \frac{R_A}{\alpha^x_{diff}}h}{\gamma - h} \tag{5}$$

Where R_L, R_{esc}, R_{cap} and R_A are, respectively the isotopic composition of the liquid water, isotopic composition of vapor escaping to the saturated layer above which is in thermodynamic equilibrium with water, isotopic composition of environmental atmospheric moisture captured by the equilibrium layer and the isotopic composition environmental atmospheric moisture. R_L, R_{esc}, R_{cap} and R_A are defined in Gonfiantini et al. (2018). α_{eq} is the isotopic fractionation factor between the liquid water and the vapor in the equilibrium layer. α_{diff} is the isotopic fractionation factor for diffusion in air affecting the vapor escaping from the equilibrium layer and the environmental vapor entering the equilibrium layer; x is the turbulent index of atmosphere.

Above the ocean one can assume that a steady state is achieved in which the isotopic composition of vapor removed from the system has same the same composition as atmospheric vapor (Merlivat, 1978). This is the global closure assumption.

$$R_A = R_{ev} \tag{6}$$

Introducing Eq. (6) in (5) gives;

$$R_{ev} = \frac{\frac{R_L}{\alpha_{eq}\alpha^x_{diff}}\gamma - \frac{R_{ev}}{\alpha^x_{diff}}h}{\gamma - h} \tag{7}$$

https://doi.org/10.5194/acp-2019-950
Preprint. Discussion started: 16 December 2019

Atmospheric Chemistry and Physics Discussions

$$R_{ev}(\gamma - h) = \frac{R_L}{\alpha_{eq}\alpha^x_{diff}}\gamma - \frac{R_{ev}}{\alpha^x_{diff}}h \tag{8}$$

$$R_{ev}(\gamma - h) + \frac{R_{ev}}{\alpha^x_{diff}}h = \frac{R_L}{\alpha_{eq}\alpha^x_{diff}}\gamma \tag{9}$$

$$R_{ev}[(\gamma - h) + \frac{h}{\alpha^x_{diff}}] = \frac{R_L}{\alpha_{eq}\alpha^x_{diff}}\gamma \tag{10}$$

$$R_{ev}[\frac{(\gamma - h)\alpha^x_{diff} + h}{\alpha^x_{diff}}] = \frac{R_L}{\alpha_{eq}\alpha^x_{diff}}\gamma \tag{11}$$

$$R_{ev} = \frac{R_L}{\alpha_{eq}\alpha^x_{diff}}\gamma[\frac{\alpha^x_{diff}}{(\gamma - h)\alpha^x_{diff} + h}] \tag{12}$$

$$R_{ev} = \frac{R_L\gamma}{\alpha_{eq}[\alpha^x_{diff}(\gamma - h) + h]} \tag{13}$$

Similarly, the global closure assumption (Eq. 6), is substituted in Eq (1) to give;

$$R_{ev} = \alpha_k.\frac{R_L.\alpha_{eq} - h.R_{ev}}{1 - h} \tag{14}$$

$$R_{ev}(1 - h) = \alpha_k.[R_L.\alpha_{eq} - h.R_{ev}] \tag{15}$$

$$R_{ev}(1 - h) + \alpha_k h.R_{ev} = \alpha_k.R_L.\alpha_{eq} \tag{16}$$

$$R_{ev}[(1 - h) + \alpha_k.h] = \alpha_k.R_L.\alpha_{eq} \tag{17}$$

$$R_{ev} = \frac{\alpha_{eq}\alpha_k R_L}{(1 - h) + \alpha_k.h]} \tag{18}$$

https://doi.org/10.5194/acp-2019-950
Preprint. Discussion started: 16 December 2019

Atmospheric Chemistry and Physics Discussions

The temperature dependent equilibrium fractionation factor is calculated using the formulation given by (Horita and Wesolowski, 1994); α_k, the kinetic fractionation factor is calculated as:

$$\alpha_k = \frac{(1-h).\theta.[\alpha_{diff}^{-x} - 1]}{1000} + 1 \tag{19}$$

The kinetic fractionation factor(α_k) takes into account diffusion in air affecting the vapor escaping from the equilibrium layer and the environmental vapor meeting at the region of equilibrium boundary layer. α_{diff} is the molecular diffusivity of the different isotopologues of water. Molecular diffusivities data are taken from three previous studies Merlivat (1978); Cappa et al. (2003); Pfahl and Wernli (2009) referred to as MJ, CD and PW respectively. x is the turbulence index of atmosphere. When $x = 1$ the vapor escapes solely by molecular diffusion and for $x = 0$ the vapor escapes only due to turbulent diffusion. θ is equal to 1 for a water body with little influence from the adjoining free troposphere but $\approx$ 0.5 for conditions over the open ocean (Gat, 2010).

Fig. 7 shows the comparison between the TCG and UCG modelled vapor isotopic composition along with our observations(Nwv). A large difference is seen between the modelled and observed isotopic composition for samples south of $\approx$ 65°S latitudes and the best match is seen for samples collected North of $\approx$ 65°S. Fig. 8 shows the correlation between the model simulations under different initial conditions and the observed isotopic composition in water vapor. It is seen that that modelled values predicts $\approx$ 50-70% of the variance recorded in the isotopic composition of the measured vapor. For Swv samples, the model fails to predict the dxs of water vapor, however, the model predicted $\delta^{18}O$ matches with the observed values.

To evaluate the performance of the prediction by these models, the slope of the dxs(model) vs relative humidity, sea surface temperature(sst) and wind speed(ws) are compared with the observed relationships. The modelled vales of the slope and intercept for the different model simulations are highly variable. Fig. 9 displays the difference between the observed and modelled values of the slope and intercept. For the dxs vs relative humidity relationship, we fail to identify any single condition which outperforms the others. However, the UCG model run for the molecular diffusivities by PW for $x = 1$ and CD for $x = 0.5$ show the smallest difference between the observed and modelled slopes and intercepts. In contrast, for the TCG simulations the least difference is for MJ and PW parameterizations for equal contribution by molecular and turbulent diffusion (i.e, $x = 0.5$). In case of dxs vs sst‘and dxs vs ws relationships, the UCG model with CD molecular diffusivities and turbulence index of 0.5 captured observed slopes and intercepts(referred to as $E_{UCG}^{CD,0.5}$ in the next section). For TCG model, while MJ with x=0.5 predicts the d vs sst relationship well, the CD molecular diffusivity ratios x=0.5 produce consistent values with the observations (Fig. 9).

Transport process further introduce mixing which allow understanding the spatial and temporal distributions of stable isotope ratios in vapor and precipitation across the sampling transect.

4.2 Understanding the equilibrium/disequilibrium

The isotopic composition of the vapor on top of the ocean is governed by the factors like wind and temperature. Fig. 10a shows the difference between the $\delta^{18}O$ isotopic composition of vapor (at equilibrium with ocean surface water) and the observed vapor isotopic composition (Δ_{eqDiff}). Kinetic fractionation and the mixing of advected vapor explains the departure from the

https://doi.org/10.5194/acp-2019-950
Preprint. Discussion started: 16 December 2019

Atmospheric Chemistry and Physics Discussions

equilibrium state. The isotopic composition of local evaporation flux is calculated based on the Unified Craig-Gordon model for CD molecular diffusivities under equal contribution by molecular and turbulent diffusion ($E_{UCG}^{CD,0.5}$). The difference between equilibrium vapor and $E_{UCG}^{CD,0.5}$ is also plotted in Fig. 10a. The calculations are done assuming the isotopic composition of the advected vapor similar to (Uemura et al., 2008) ($\delta^2H \approx$-109‰) from 31°S to 65°S i.e. in the region where westerlies dominates. For samples collected in the polar ocean south of 65°S the temperatures are a limiting factor for the evaporation process to happen and hence the large differences from the equilibrium conditions can be explained by invoking the process of mixing of Antarctic vapor which gets transported to the sites by the polar easterlies. Taking the average isotopic composition of water vapor collected at Dome C site (Dec 2014-Jan) (Wei et al., 2019) (δ^2H= -490 $\pm$ 23‰). It is seen that in order to explain the water vapor isotope ratio observation over the ocean south of 65°S the contribution of depleted Antarctic vapor. Fig. 10b shows the relative contribution of advected and locally generated moisture. The advected component is a prominent component of the ambient vapor and its contribution becomes greater with increasing latitudes. South of 65°S the amount of moisture present in the atmosphere is less and is majorly local in origin with a small mixing of heavily depleted Antarctic vapors.

5 Conclusions

The isotopic composition of evaporating vapor is governed by the isotopic composition of the water, ambient vapor isotopic composition, exchange and mixing processes at the water-air interface as well as the local meteorological conditions. These controlling parameters were considered separately or simultaneously for quantification of evaporation using the Craig-Gordon models. In this study, we measured the isotopic composition of water vapor over the ocean and surface water samples collected across a latitudinal transect from Mauritius to Prydz. The Traditional (Craig and Gordon, 1965) (TCG) and the Unified C-G (UCG) (Gonfiantini et al., 2018) equations were tested to predict the isotopic composition of evaporation flux across the Southern Ocean incorporating different molecular diffusivity ratios for varying fractions of molecular and turbulent diffusion. $E_{UCG}^{CD,0.5}$ i.e. the UCG model with molecular diffusivity ratios proposed by Cappa et al. (2003), predicted the slope and the intercepts of dxs vs meteorological parameters with an appreciable accuracy and consistent with our observation. The relative contribution of advected and evaporated fluxes was estimated by assigning end member isotopic composition and solving in a two-component mixing framework. The $E_{UCG}^{CD,0.5}$ provides best approximation of the locally generated end member composition and the advected moisture flux is assigned values based on the origin and path followed by the back trajectories. We found that beyond 65S latitude lighter isotope values observed in the water can be explained by invoking mixing of Antarctic vapor with linearly increasing contribution towards the coast.

Author contributions

SSD and PG conceptualized the study. SSD and AS performed the sample collection and analysis. SSD wrote the paper and PG supervised the study. AK provided the resources during the expeditions.

https://doi.org/10.5194/acp-2019-950
Preprint. Discussion started: 16 December 2019

Atmospheric Chemistry and Physics Discussions

Acknowledgements

We would like to thank the Ministry of Earth Sciences, Government of India, the National Centre for Polar and Ocean Research, Goa, India and members of the Scientific Southern Ocean Expeditions.

Data Availability

The data that support the findings of this study have been uploaded as a supplementary document.

Declaration of interests

The authors declare that they have no known competing financial interests or personal relationships that could have appeared to influence the work reported in this paper.

https://doi.org/10.5194/acp-2019-950
Preprint. Discussion started: 16 December 2019

Atmospheric Chemistry and Physics Discussions

References

Araguás-Araguás, L., Froehlich, K., and Rozanski, K.: Deuterium and oxygen-18 isotope composition of precipitation and atmospheric moisture, Hydrological Processes, 14, 1341–1355, 2000.

Benetti, M., Reverdin, G., Pierre, C., Merlivat, L., Risi, C., Steen-Larsen, H. C., and Vimeux, F.: Deuterium excess in marine water vapor: Dependency on relative humidity and surface wind speed during evaporation, Journal of Geophysical Research: Atmospheres, 119, 584–593, 2014.

Benetti, M., Aloisi, G., Reverdin, G., Risi, C., and Sèze, G.: Importance of boundary layer mixing for the isotopic composition of surface vapor over the subtropical North Atlantic Ocean, Journal of Geophysical Research: Atmospheres, 120, 2190–2209, 2015.

Benetti, M., Reverdin, G., Aloisi, G., and Sveinbjörnsdóttir, Á.: Stable isotopes in surface waters of the Atlantic Ocean: Indicators of ocean-atmosphere water fluxes and oceanic mixing processes, Journal of Geophysical Research: Oceans, 122, 4723–4742, 2017a.

Benetti, M., Steen-Larsen, H. C., Reverdin, G., Sveinbjörnsdóttir, Á. E., Aloisi, G., Berkelhammer, M. B., Bourlès, B., Bourras, D., De Coetlogon, G., Cosgrove, A., et al.: Stable isotopes in the atmospheric marine boundary layer water vapour over the Atlantic Ocean, 2012–2015, Scientific data, 4, 160 128, 2017b.

Cappa, C. D., Hendricks, M. B., DePaolo, D. J., and Cohen, R. C.: Isotopic fractionation of water during evaporation, Journal of Geophysical Research: Atmospheres, 108, 2003.

Chahine, M. T.: The hydrological cycle and its influence on climate, Nature, 359, 373, 1992.

Craig, H.: Isotopic variations in meteoric waters, Science, 133, 1702–1703, 1961.

Craig, H. and Gordon, L. I.: Deuterium and oxygen 18 variations in the ocean and the marine atmosphere, 1965.

Dansgaard, W.: Stable isotopes in precipitation, Tellus, 16, 436–468, 1964.

Draxler, R. R. and Hess, G.: An overview of the HYSPLIT_4 modelling system for trajectories, Australian meteorological magazine, 47, 295–308, 1998.

Galewsky, J., Steen-Larsen, H. C., Field, R. D., Worden, J., Risi, C., and Schneider, M.: Stable isotopes in atmospheric water vapor and applications to the hydrologic cycle, Reviews of Geophysics, 54, 809–865, 2016.

Gat, J.: Isotope hydrology: a study of the water cycle, vol. 6, World scientific, 2010.

Gat, J., Klein, B., Kushnir, Y., Roether, W., Wernli, H., Yam, R., and Shemesh, A.: Isotope composition of air moisture over the Mediterranean Sea: an index of the air–sea interaction pattern, Tellus B, 55, 953–965, 2003.

Gat, J. R.: Oxygen and hydrogen isotopes in the hydrologic cycle, Annual Review of Earth and Planetary Sciences, 24, 225–262, 1996.

Gonfiantini, R., Wassenaar, L. I., Araguas-Araguas, L., and Aggarwal, P. K.: A unified Craig-Gordon isotope model of stable hydrogen and oxygen isotope fractionation during fresh or saltwater evaporation, Geochimica et Cosmochimica Acta, 235, 224–236, 2018.

Horita, J. and Wesolowski, D. J.: Liquid-vapor fractionation of oxygen and hydrogen isotopes of water from the freezing to the critical temperature, Geochimica et Cosmochimica Acta, 58, 3425–3437, 1994.

Kanamitsu, M., Ebisuzaki, W., Woollen, J., Yang, S.-K., Hnilo, J., Fiorino, M., and Potter, G.: Ncep–doe amip-ii reanalysis (r-2), Bulletin of the American Meteorological Society, 83, 1631–1643, 2002.

Korzoun, V. and Sokolov, A.: World water balance and water resources of the earth, Water Development, Supply and Management (UK)(USA)(Canada)(Australia)(France)(Germany, FR), 1978.

Merlivat, L.: Molecular diffusivities of H 2 16 O, HD 16 O, and H 2 18 O in gases, The Journal of Chemical Physics, 69, 2864–2871, 1978.

https://doi.org/10.5194/acp-2019-950
Preprint. Discussion started: 16 December 2019

Atmospheric Chemistry and Physics Discussions

Midhun, M., Lekshmy, P., and Ramesh, R.: Hydrogen and oxygen isotopic compositions of water vapor over the Bay of Bengal during monsoon, Geophysical Research Letters, 40, 6324–6328, 2013.

Noone, D. and Sturm, C.: Comprehensive dynamical models of global and regional water isotope distributions, in: Isoscapes, pp. 195–219, Springer, 2010.

Oki, T. and Kanae, S.: Global hydrological cycles and world water resources, science, 313, 1068–1072, 2006.

Pfahl, S. and Wernli, H.: Lagrangian simulations of stable isotopes in water vapor: An evaluation of nonequilibrium fractionation in the Craig-Gordon model, Journal of Geophysical Research: Atmospheres, 114, 2009.

Prasanna, K., Ghosh, P., Bhattacharya, S., Rahul, P., Yoshimura, K., and Anilkumar, N.: Moisture rainout fraction over the Indian Ocean during austral summer based on 18O/16O ratios of surface seawater, rainwater at latitude range of 10 N-60 S., Journal of Earth System Science, 127, 2018.

Rahul, P., Ghosh, P., Bhattacharya, S., and Yoshimura, K.: Controlling factors of rainwater and water vapor isotopes at Bangalore, India: Constraints from observations in 2013 Indian monsoon, Journal of Geophysical Research: Atmospheres, 121, 2016.

Rahul, P., Prasanna, K., Ghosh, P., Anilkumar, N., and Yoshimura, K.: Stable isotopes in water vapor and rainwater over Indian sector of Southern Ocean and estimation of fraction of recycled moisture, Scientific reports, 8, 2018.

Rangarajan, R. and Ghosh, P.: Role of water contamination within the GC column of a GasBench II peripheral on the reproducibility of 18O/16O ratios in water samples, Isotopes in environmental and health studies, 47, 498–511, 2011.

Schmidt, G., Bigg, G., and Rohling, E.: Global seawater oxygen-18 database–v1. 21, Online at http://data. giss. nasa. gov/o18data, online at http://data. giss. nasa. gov/o18data, 1999.

Shiklomanov, I. A.: World water resources: a new appraisal and assessment for the 21st century: a summary of the monograph World water resources, Unesco, 1998.

Srivastava, R., Ramesh, R., Prakash, S., Anilkumar, N., and Sudhakar, M.: Oxygen isotope and salinity variations in the Indian sector of the Southern Ocean, Geophysical Research Letters, 34, 2007.

Stein, A., Draxler, R., Rolph, G., Stunder, B., Cohen, M., and Ngan, F.: NOAA's HYSPLIT atmospheric transport and dispersion modeling system, Bulletin of the American Meteorological Society, 96, 2059–2077, 2015.

Tiwari, M., Nagoji, S. S., Kartik, T., Drishya, G., Parvathy, R., and Rajan, S.: Oxygen isotope salinity relationships of discrete oceanic regions from India to Antarctica vis a vis surface hydrological processes, Journal of Marine Systems, 113, 88–93, 2013.

Uemura, R., Matsui, Y., Yoshimura, K., Motoyama, H., and Yoshida, N.: Evidence of deuterium excess in water vapor as an indicator of ocean surface conditions, Journal of Geophysical Research: Atmospheres, 113, 2008.

Wei, Z., Lee, X., Aemisegger, F., Benetti, M., Berkelhammer, M., Casado, M., Caylor, K., Christner, E., Dyroff, C., García, O., et al.: A global database of water vapor isotopes measured with high temporal resolution infrared laser spectroscopy, Scientific data, 6, 180 302, 2019.

Yoshimura, K.: Stable water isotopes in climatology, meteorology, and hydrology: A review, Journal of the Meteorological Society of Japan. Ser. II, 93, 513–533, 2015.

https://doi.org/10.5194/acp-2019-950
Preprint. Discussion started: 16 December 2019

Atmospheric Chemistry and Physics Discussions

Table 1. Descriptive statistics of the water vapor isotopic composition

	$\delta^{18}O(‰)$	$\delta^{2}H(‰)$	**dxs**$(‰)$
SOE IX Water Vapor(n=34)			
Max	-10.86	-80.79	18.65
Min	-27.47	-221.38	-8.37
Mean(Stdev)	-16.96($\pm$5.25)	-130.35($\pm$44.43)	5.35($\pm$8.06)
SOE X Water Vapor(n=37)			
Max	-11.46	-88.03	14.54
Min	-21.18	-163.28	-23.71
Mean(Stdev)	-15.77($\pm$2.53)	-126.07($\pm$20.23)	0.08($\pm$8.46)
SOE X Water Vapor (S) (n=19)			
Max	-11.26	-88.08	32.29
Min	-21.45	-163.75	-23.75
Mean(Stdev)	-16.79($\pm$3.04)	-129.69($\pm$23.51)	4.65($\pm$12.83)

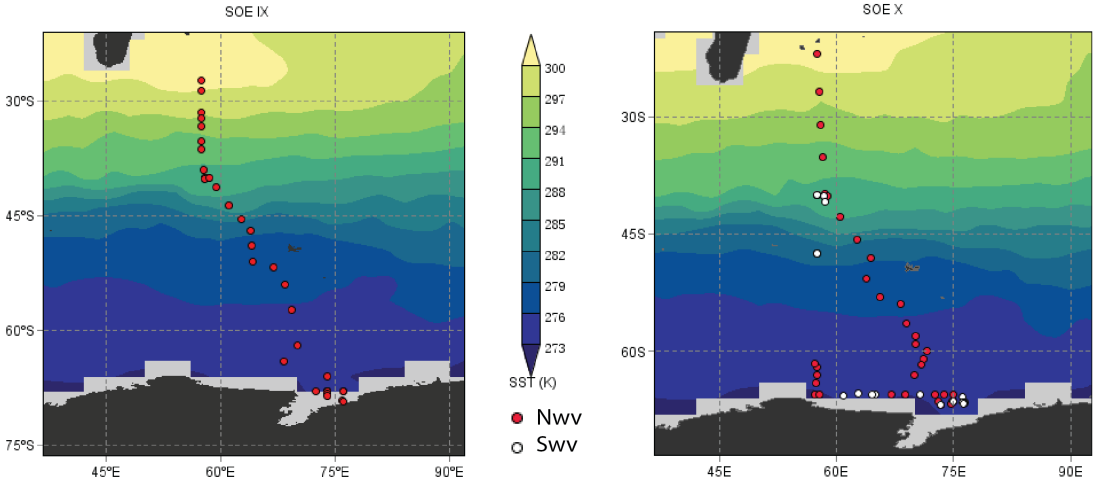

Figure 1. The sample collection locations overlain on a map of mean monthly sst (^oK) during the two expeditions. The locations of water vapor samples (Nwv and Swv) collected are depicted as circles.

https://doi.org/10.5194/acp-2019-950
Preprint. Discussion started: 16 December 2019

Atmospheric Chemistry and Physics Discussions

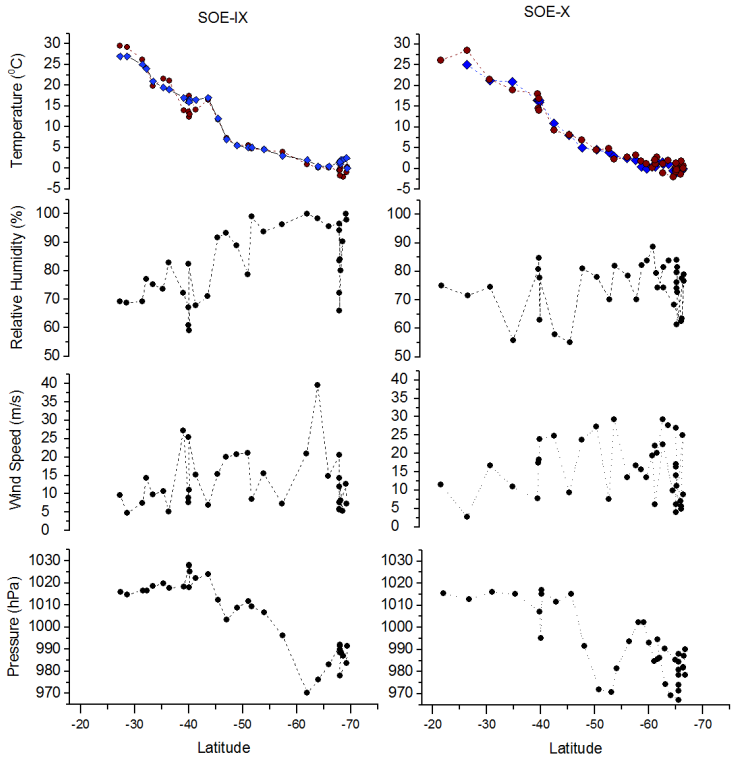

Figure 2. Latitudinal variability of measured meteorological parameters, air temperature, relative humidity, wind speed and atmospheric pressure. Red and blue colors in the temperature plots depict air temperature and sea surface temperature.

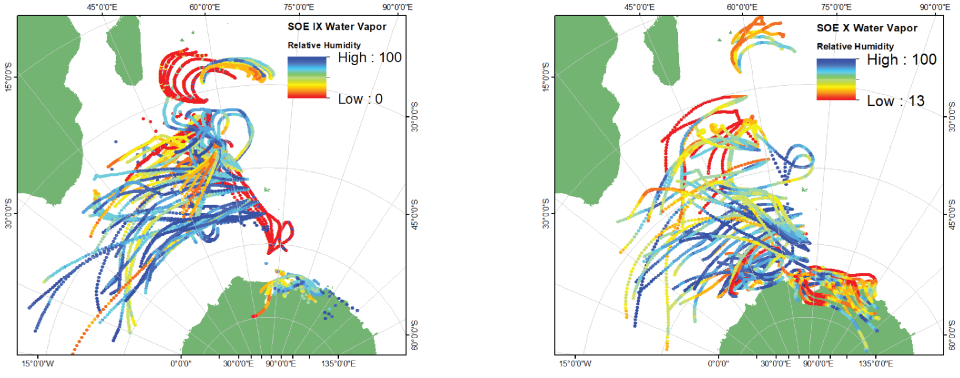

Figure 3. shows 72 hours back trajectories calculated using HYSPLIT with Reanalysis II as forcing. The trajectories shown are for three heights surface, 500m and 1500m above the mean sea level and the colors depict the variation of relative humidity along the trajectories.

https://doi.org/10.5194/acp-2019-950
Preprint. Discussion started: 16 December 2019

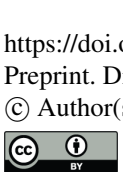

Atmospheric Chemistry and Physics Discussions

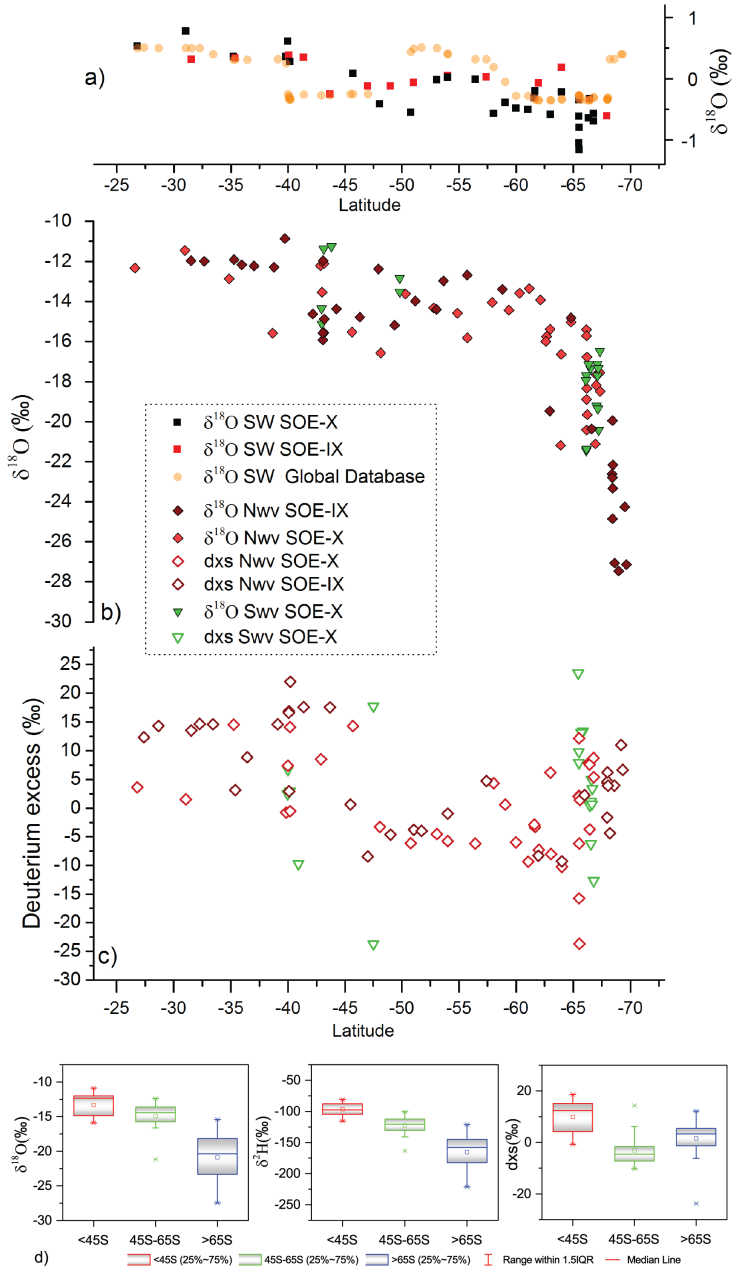

Figure 4. a) Shows the measured $\delta^{18}O_{SW}$ and from a global sea water $\delta^{18}O_{SW}$ database of surface water along the latitudinal transect b) Latitudinal variability in water vapor and surface water samples collected samples collected during the two expeditions. Light and dark red filled diamonds depict the $\delta^{18}O_{WV}$ of water vapor samples collected during the two expeditions at height of ≈ 15m above the water surface. Filled green triangles depict the samples collected close to the air-water interface during calm ocean conditions. c) shows the latitudinal variation of dxs in water vapor and precipitation samples collected for samples d) Zonal variation of $\delta^{18}O$,$\delta^{2}H$ and dxs along the latitudinal transect.

https://doi.org/10.5194/acp-2019-950
Preprint. Discussion started: 16 December 2019

Atmospheric Chemistry and Physics Discussions

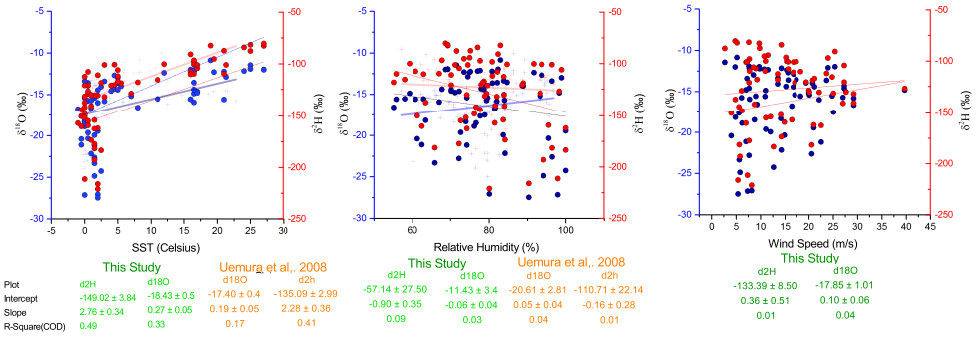

(a) All Nwv samples

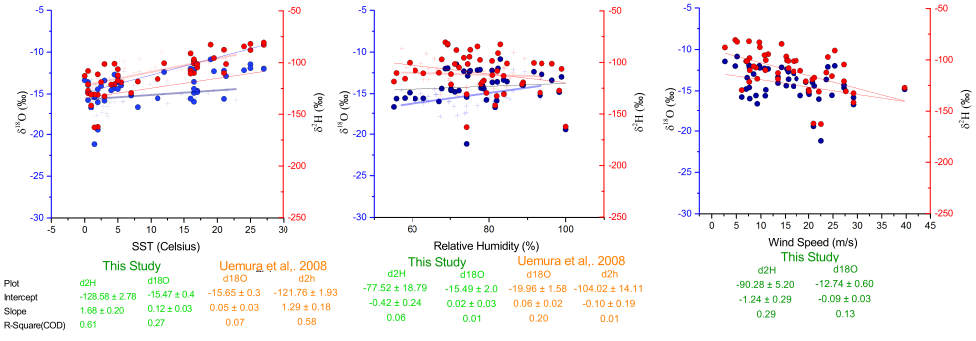

(b) Water vapor samples south of 65°S

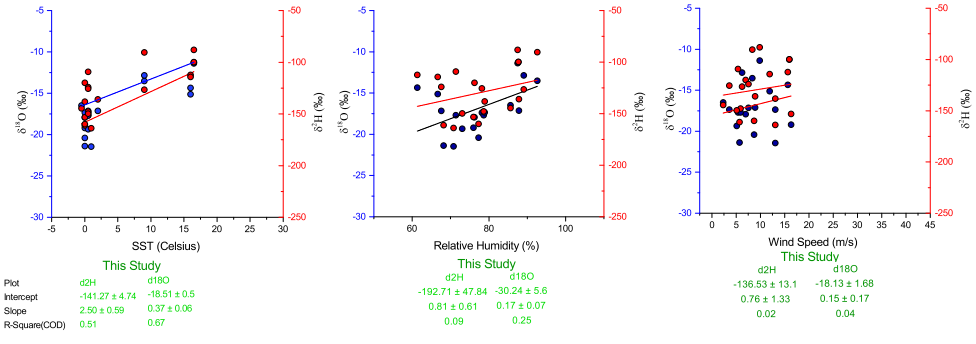

(c) All Swv samples

Figure 5. Linear regression equations for isotopic composition of water vapor and physical parameters(sea surface temperature, relative humidity and wind speed. Filled blue and red circles depict the $\delta^{18}O$ and $\delta^{2}H$ respectively. The linear regression lines are shown as dotted red and blue for $\delta^{2}H$ and $\delta^{18}O$ respectively. The data from Uemura et al. (2008) are plotted as watermarks with red and blue colors representing $\delta^{2}H$ and $\delta^{18}O$ respectively

https://doi.org/10.5194/acp-2019-950
Preprint. Discussion started: 16 December 2019

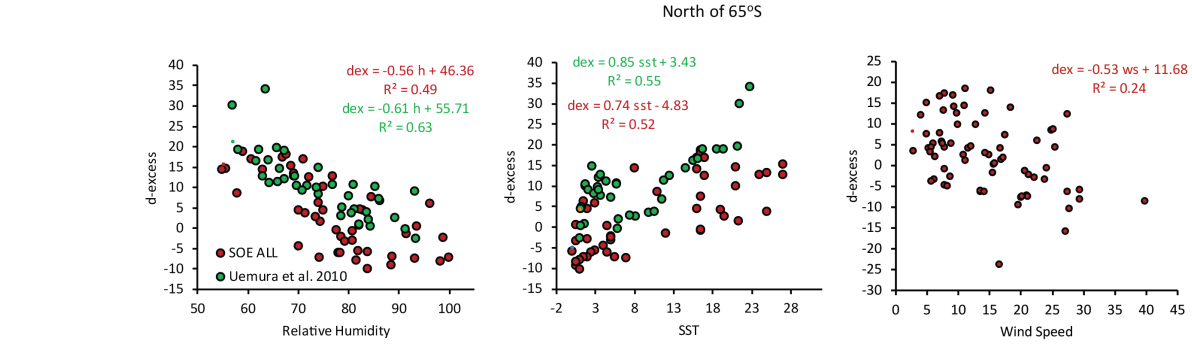

Figure 6. Relationship between dxs in water vapor and the meteorological conditions (relative humidity, sea surface temperature and wind speed). Also plotted along is the data from Uemura et al. (2008)shown as filled green circles.

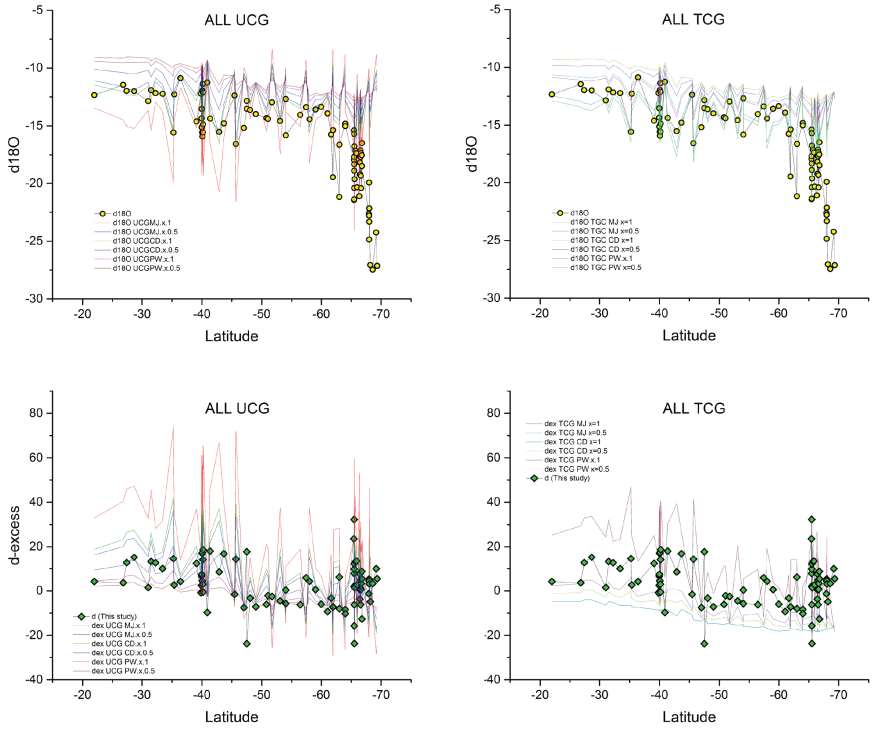

Figure 7. Comparison between the latitudinal distribution of the measured water vapor $\delta^{18}O$ (yellow diamonds), dxs (green diamonds) and predicted by the TCG and UCG models for different molecular diffusivity ratios and ocean surface conditions (i.e. the fraction of molecular to turbulent diffusion)

https://doi.org/10.5194/acp-2019-950
Preprint. Discussion started: 16 December 2019

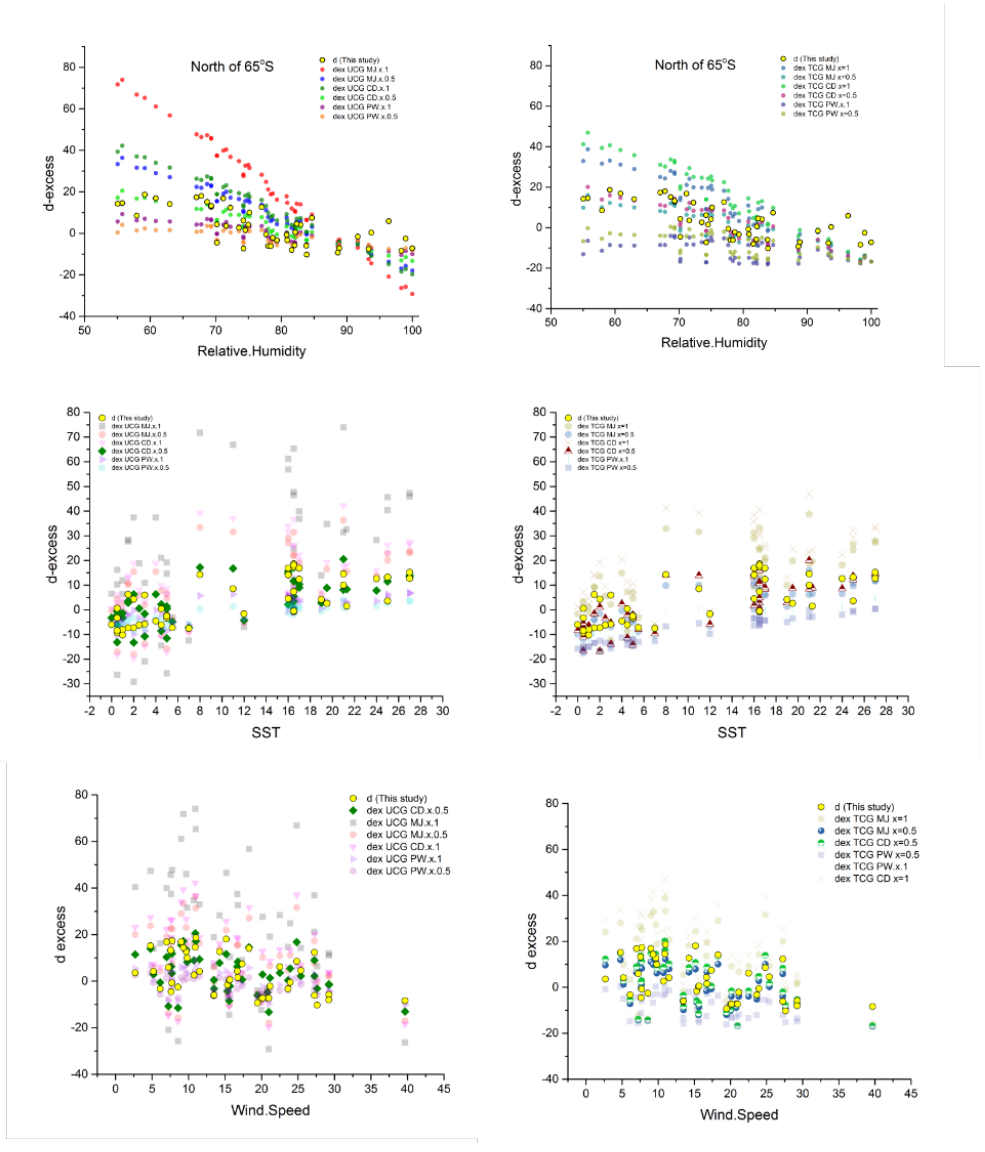

Figure 8. Depicts the relationship between dxs and the local meteorological parameters observed (yellow circles) and predicted by the UCG (left column) and TCG models for different molecular diffusivity ratios and turbulence of the ocean.

https://doi.org/10.5194/acp-2019-950
Preprint. Discussion started: 16 December 2019

Atmospheric Chemistry and Physics Discussions

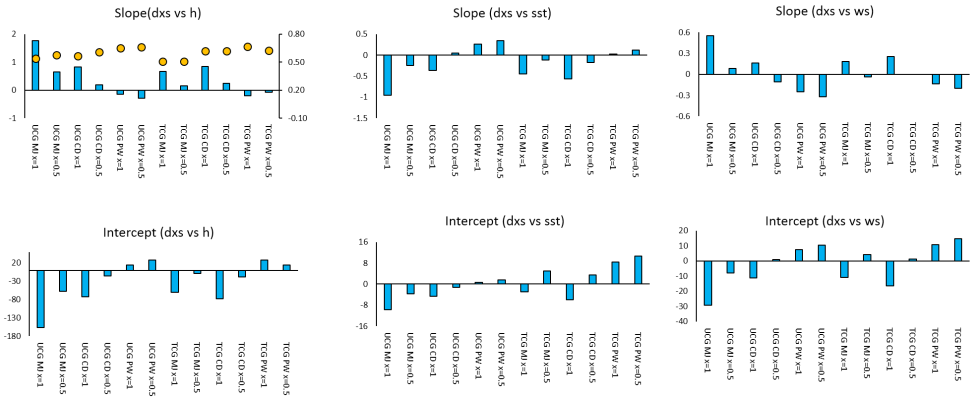

Figure 9. Differences between observed and predicted slopes and intercepts of the relationships between dxs vs h, sst and ws. The orange circles in the first plot depict the correlation between the observed and various model simulations.

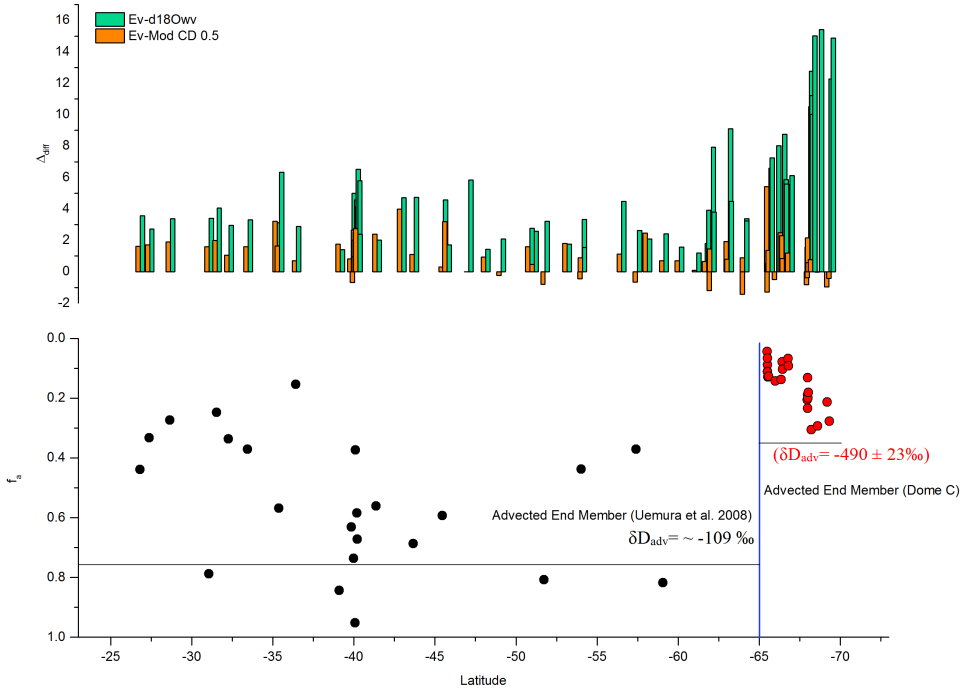

Figure 10. a) depicts the difference between the equilibrium vapor and the modelled, observed water vapor isotopic composition Fraction of advected vapor that explains the water vapor isotopic composition.